Electric Field Mapping System Using an Optical-Fiber-Based Electrooptic Probe

K. Yang, Linda P. B. Katehi, *Fellow, IEEE*, and J. F. Whitaker

Abstract—A microwave electric-field mapping system based on electrooptic sampling has been developed using micromachined GaAs crystals mounted on gradient index lenses and single-mode optical fibers. The probes are able to detect three orthogonal polarizations of electric fields and, due to the flexibility and size of the optical fiber, can be positioned not only from the extreme near-field to the far-field regions of microwave and millimeter-wave structures, but also inside of enclosures such as waveguides and packages.

Index Terms—Electric-field measurement, electrooptic sampling, far-field radiation patterns, near-field radiation patterns.

I. INTRODUCTION

ELECTRO-OPTIC (EO) field mapping is becoming recognized as a promising diagnostic measurement technique for the microwave and millimeter-wave regimes. Due to its single-micrometer spatial-resolution, broad bandwidth, and low invasiveness, EO field mapping has been utilized for fault isolation of microwave integrated circuits [1] and extreme near-field mapping and performance testing of various active and passive antennas and arrays [2]. Based on the initial embodiment of the EO field-mapping system, where both the detection and signal laser beams traveled in open air [3] and for which applications have been limited to exposed, planar structures, a new field-mapping system has now been developed using fiber-mounted, micromachined GaAs crystals as the electric-field sensors. Due to the flexibility of the optical fiber and the small size of a micromachined GaAs tip, the fiber-based electrooptic probes may be inserted into enclosures such as waveguides and packages in order to measure electric fields. A similar concept for a fiber-based electrooptic sensor has been recently demonstrated in measurements of 1-GHz microwave signals [4]. However, the use of such a probe for phase measurements, measurements inside of a microwave package, high-frequency (Ka-band) microwave signal measurements, and the characterization of three orthogonal field components have not been reported until now.
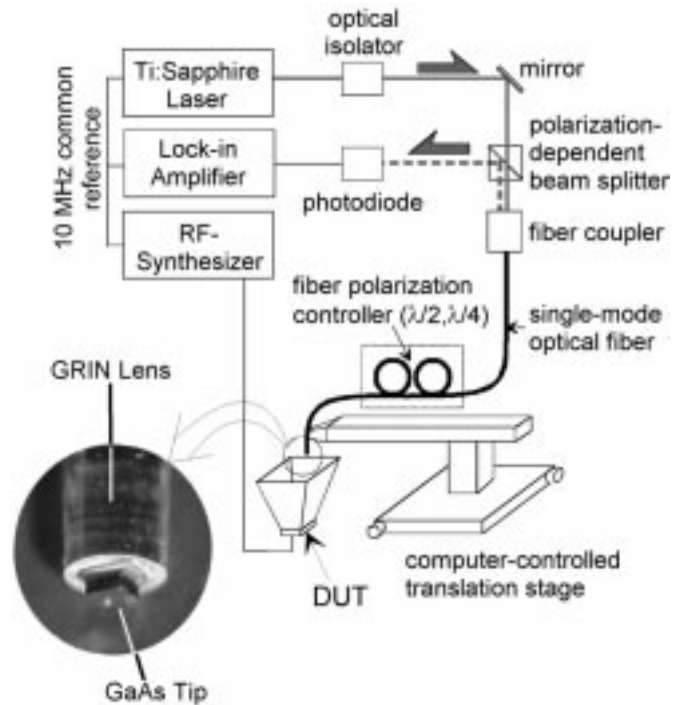
Fig. 1. Fiber-based EO-field-mapping system schematic. The input and output (signal) beams are displayed with solid and dashed gray lines, respectively. A magnified photo of the GaAs probe tip including the GRIN lens is shown.

II. MEASUREMENT SETUP CONFIGURATION

Fig. 1 is a schematic diagram of the fiber-based EO sampling system utilized in this work. In general, the optical pulse-train from a phase-stabilized, mode-locked laser (100-fs-duration pulses; 80-MHz pulse repetition rate) is modulated via the Pockels effect in the GaAs electrooptic crystal by the RF field to be imaged. The laser wavelength is tuned to 900 nm and the average input power to the fiber is attenuated to around 15 mW to avoid absorption by the GaAs [5]. This differs from previous work on GaAs electrooptic field imaging [6] in that the probe tip is now integrated with an optical fiber, vastly improving the positioning ability of the probe and the optical coupling. The polarization-dependent beam-splitter limits the optical transmission to one particular polarization, and this beam is focused into the single-mode optical fiber using a commercial fiber-coupler. A gradient-index (GRIN) lens with diameter of 1.0 mm and length of 5.0 mm is mounted at the opposite end of the fiber to focus the beam onto the surface of the GaAs crystal, which is attached to the GRIN lens using transparent cement. In order to align the linear polarization of the laser to the optic axis of the GaAs and to manipulate the elliptical polarization of the light returning

from the probe, two polarization-controlling loops are introduced into the fiber to serve as half- and quarter-wave plates.

The beam reflected from the probe contains the electrooptic signal, modulated by the RF electric field so that it possesses an additional polarization angle, δ. The signal beam is rerouted to the photodiode by the beam splitter, which also converts δ into an intensity change, and the optical signal is transformed into an electrical signal via the photodiode.

The GaAs tips, with 500×500-μm footprint area and 200-μm thickness, have a high-reflection optical coating deposited on their exposed surface. A $\langle 100 \rangle$ orientated GaAs tip was used as the EO crystal to detect the normal electric field component (i.e., relative to the device under test [DUT]), while $\langle 110 \rangle$ GaAs was used to sense tangential fields. The orthogonal tangential fields are distinguished by rotating the relative orientation between the $\langle 110 \rangle$ GaAs tip and the DUT by $90°$.

The sensor end of the fiber is attached to a supporting arm mounted on the computer controlled X–Y translation stage to allow the fiber-mounted probe to be scanned in two directions. All the materials around the sensor area, including the GRIN lens and fiber, have permittivities around 4, except for the GaAs tip itself, which has ε_r of 12, much lower than nearly all conventional EO crystals by more than a factor of 3. Thus the fiber-based system can be expected to reduce any effect of the sensor on the DUT significantly. Furthermore, the measurement flexibility is dramatically improved since the probe may be freely positioned without restrictions arising from the placement of the other optical components or the DUT.

The input RF frequency to the DUT is selected to be an integer multiple of the pulse repetition rate of the laser (80 MHz) plus an additional offset frequency (3.0 MHz). Using harmonic mixing, the lock-in amplifier receives the 3-MHz intermediate frequency arising from the difference signal between the synthesizer input and the laser-harmonic local oscillator. A computer records the amplitude and phase of the IF at each measurement point.

III. MEASUREMENT RESULTS

In order to demonstrate the versatility of the fiber-based EO field-mapping system, the normal electric field component inside of a shielded microstrip transmission line, which may not be obtained by any other measurement method, including free-space EO field mapping, was imaged using the $\langle 100 \rangle$-oriented GaAs probe tip. This field pattern was then compared with the field distribution from an identical microstrip without a shielding cavity. For the measurement, a 50-Ω microstrip transmission line was fabricated on a duroid substrate with 75-mil thickness and a dielectric constant (ε_r) of 6.15. The output port of the microstrip was short-terminated in order to provide a standing wave pattern.

The height of the cavity wall was 6.0 mm above the top surface of the microstrip. In order for the probe tip to have freedom of movement in three dimensions in the closed metal cavity, an oversized sliding top metal plate was employed to complete the enclosure. A 2-mm diameter access hole in the sliding top plate allowed the EO probe to be positioned inside of the cavity as shown in Fig. 2. Since the top plate and the fiber-based EO probe were mechanically connected to the x–y translation stage,
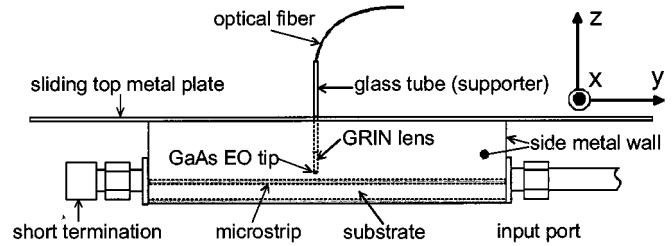

Fig. 2. Side view of the shielded microstrip line with fiber-based EO probe. The top slide plate is connected to a computer-controlled x–y translation stage in order to achieve 2-D movement.
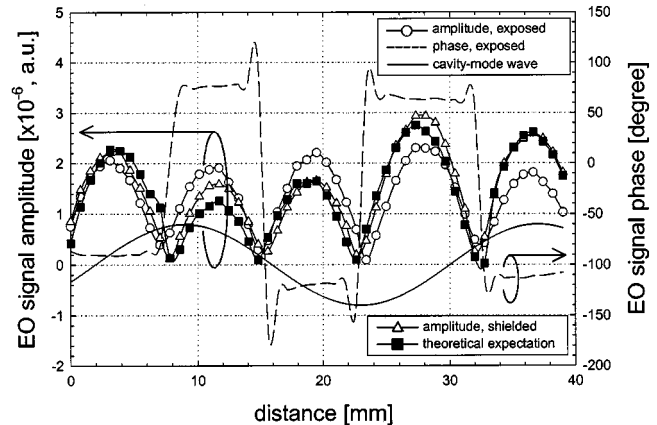

Fig. 3. Amplitude and phase of standing waves from open and shielded microstrip, including the exposed microstrip result superimposed with the cavity mode calculation.

the probe could scan a two-dimensional (2-D) field distribution from the interior of the cavity, while the top plate maintained electrical contact to the cavity walls. In addition to the 2-D (i.e., x–y plane) field mapping capability, the vertical position (z-direction) of the probe could be adjusted externally.

For both exposed and shielded microstrip, the normal electric fields were measured at distances of 1.0, 2.5, and 5.0 mm from the top of the microstrip surface. The scanning window was 2.9 cm (x) by 3.9 cm (y), using the step sizes (and thus also the spatial resolutions) of 580 μm (x) and 780 μm (y). Each field map was acquired in approximately 15 min.

The results show typical standing wave patterns that have periodic peaks with $180°$ phase changes. The separation between the peaks on the microstrip was 0.87 mm, which shows excellent agreement with the theoretically expected peak-to-peak distance. The peak amplitudes were reduced by 16 dB as the measurement distance increased from 1.0 mm to 5.0 mm for the exposed microstrip.

While 2-D field maps were extracted at all three measurement heights, in Fig. 3 we show only the one-dimensional comparison between the exposed and shielded microstrip along the centerlines at a 1.0-mm height. The phase shows virtually identical changes of $180°$ for each amplitude peak. However, a nonuniform amplitude distribution is observed on the shielded microstrip, while the exposed microstrip exhibits a reasonably uniform peak amplitude distribution. Since the geometries of the two microstrips (including the size of the substrate) are identical, the most plausible explanation for the

amplitude discrepancy is the existence of a cavity-mode wave. The cavity mode wave was thus calculated based on the cavity resonator theory, and the effect of the microstrip substrate was taken into account using the cavity perturbation theory [7]. Superimposing the calculated cavity standing wave pattern on the exposed microstrip result demonstrates that our cavity measurement accurately reveals the effect of the enclosure on the microstrip.

While the 2-D field images of relatively simple structures could also be computed using numerical full-wave analysis methods, this striking experimental example shows that the actual field patterns can be extracted from a package for the purposes of fault analysis or to diagnose sources of cross-talk or interference that are not quickly or easily computed.

In order to demonstrate the application of this fiber-based field-mapping probe to radiating waves, and also to utilize its transverse-field measurement capability, the dominant electric field component of the Ka-band horn was scanned using a $\langle 110 \rangle$ GaAs probe tip both in the aperture plane (plane A) and in a plane that was two wavelengths from the aperture within the interior of the horn (plane B). The scanning areas were 3.39 cm $\times$ 5.57 cm for plane A and 2.78 cm $\times$ 4.17 cm for plane B, with plane B being reduced in size due to the natural taper of the microwave horn antenna. Fifty scanning steps were used for both the x- and y-directions, with a single scan taking approximately 30 min.

The results indicate, as expected, that there is a more uniform field distribution for both amplitude and phase at the aperture, while the wave front is quite curved inside of the horn cavity. Specifically, the phase of the field at the aperture has an almost uniform distribution, while it displays about a 50° phase variation across the scanned area along the y-axis on the plane B.

IV. CONCLUSION

A fiber-based electrooptic field mapping system has been developed using micromachined GaAs probe tips. The fiber-based system has lower permittivity than other scanning field probes, provides excellent measurement flexibility so that the scanning can be performed at any arbitrary orientation, and allows insertion of the field sensor into microwave enclosures and packages. In particular, the fiber-based EO field mapping system makes it possible to extract electric field distributions of complicated micro- and millimeter wave circuits shielded by metal walls. The fiber-based EO system can be applied to the design, characterization, and failure analysis of quasioptical power-combining arrays, power amplifiers, and other microwave and millimeter wave systems.

REFERENCES

[1] K. Yang, G. David, S. Robertson, J. F. Whitaker, and L. P. B. Katehi, "Electrooptic mapping of near field distributions in integrated microwave circuits," *IEEE Trans. Microwave Theory Tech.*, vol. 46, pp. 2338–2343, Dec. 1998.

[2] K. Yang, G. David, W. Wang, T. Marshall, L. W. Pearson, Z. Popovic, L. P. B. Katehi, and J. F. Whitaker, "Electrooptic field mapping of quasioptic power-combining arrays," in *Ultrafast Electronics and Optoelectronics Conference*, ser. Technical Digest.   Washington, DC: Opt. Soc. Amer., 1999, pp. 30–32.

[3] J. A. Valdmanis and G. Mourou, "Subpicosecond electrooptic sampling: Principles and applications," *IEEE J. Quantum Electron.*, vol. QE-22, pp. 69–78, Jan. 1986.

[4] S. Wakana, T. Ohara, M. Abe, E. Yamazaki, M. Kishi, and M. Tsuchiya, "Novel electromagnetic field probe using electro-flash magneto-optical crystals mounted on optical-fiber facets for microwave circuit diagnostics," in *IEEE International Microwave Symposium Digest*.   Piscataway, NJ: IEEE Press, 2000, p. 1615.

[5] B. H. Kolner and D. M. Bloom, "Electrooptic sampling in GaAs integrated circuits," *IEEE J. Quantum Electron.*, vol. QE-22, pp. 79–93, Jan. 1986.

[6] K. Yang, L. P. B. Katehi, and J. F. Whitaker, "Electrooptic field mapping utilizing external Gallium Arsenide probes," *Appl. Phys. Lett.*, vol. 77, no. 4, pp. 486–488, July 2000.

[7] D. M. Pozar, *Microwave Engineering*. Reading, MA: Addison-Wesley, 1990.